Global and Planetary Change 92–93 (2012) 30–39

Contents lists available at SciVerse ScienceDirect

Global and Planetary Change

journal homepage: www.elsevier.com/locate/gloplacha

Glacial lake distribution in the Mount Everest region: Uncertainty of measurement and conditions of formation

Franco Salerno [a,b,*], Sudeep Thakuri [a,b], Carlo D'Agata [b,c], Claudio Smiraglia [b,c], Emanuela Chiara Manfredi [a,b], Gaetano Viviano [a,b], Gianni Tartari [a,b]

[a] Water Research Institute, National Research Council (IRSA-CNR), Via del Mulino 19, Brugherio (MB) 20861, Italy
[b] Ev-K2-CNR Committee, Via San Bernardino, 145, Bergamo 24126, Italy
[c] Department of Earth Sciences "Ardito Desio", University of Milan, Italy

ARTICLE INFO

Article history:
Received 22 April 2011
Accepted 4 April 2012
Available online 13 April 2012

Keywords:
ALOS
Supraglacial lakes
Proglacial lakes
Mount Everest
Accuracy
Glacier distribution

ABSTRACT

This study provides a complete mapping (October 2008) of glacial lakes and debris-covered glaciers in the Mount Everest region. These types of analyses are essential in studies of the impact of recent climate change, and therefore the uncertainty of measurements is discussed with the aim of creating a reference study for use when glaciers and lakes are delineated using remote sensing imagery. Moreover, attention is focused on conditions related to the formation of lakes, which is the greatest evidence of the impact of climate change at high altitudes characterized by debris-covered glaciers. Regarding the formation process of *supraglacial lakes*, our findings confirm that the slope of the glacier where lakes are located is primarily responsible for the low flow velocity of this zone. Otherwise, this study is novel in its identification of a further boundary condition. The slope of the glacier upstream is able to influence both the low flow velocity and the high ablation rates at the glacier terminus. In fact, the imbalance between the two glacier zones generates the downslope passage of debris, snow and ice. We found the slope of the glacier upstream to be inversely correlated with the relevant total surface of the lakes downstream. The multiple regression model developed in this study, considering the slopes of the two glacier areas distinctly, has been able to predict 90% of the *supraglacial lake* surfaces. Concerning the surfaces of lakes not directly connected with glaciers (*unconnected glacial lakes*), we found they are correlated with the dimensions of their drainage basin, whereas no correlation was found with the glacier cover in the basin. Considering that the evaporation/precipitation ratio at these altitudes is approximately 0.34, the evolution of these lakes appears to be a helpful sign for detecting the precipitation trend of these high-altitude regions.

1. Introduction

Scherler et al. (2011) provide a comprehensive study along the entire Hindu Kush-Himalaya range underlining the non-uniform response of glaciers to climate change. In particular, the study highlights the importance of debris cover for understanding glacier evolution, an effect that has so far been neglected in predictions of future water availability. The southern central Himalayas are the region with glaciers that presents the highest debris coverage. Supraglacial debris cover influences the terminus dynamics and can thereby modify a glacier's response to climate change. Supplementary material 1 describes previous studies on glacier and lake distribution in the Mount Everest region. Recent studies in this region have found several debris-covered glaciers with stagnant ice in the glacier termini (Scherler et al., 2008; Quincey et al., 2009). Although surface lowering indicates that such glaciers are currently shrinking, their fronts remain remarkably stable. The retreat rate of a debris-covered glacier is thus unsuitable as an indicator of recent climate change (Scherler et al., 2011). Moreover, Jacobs et al. (2012) note that the high mountains of Asia are subject to a mass loss for the years 2003 through 2010 at a level that is significantly lower (4 ± 20 Gt yr^{-1}) than previous estimates (47 to 55 ± 20 Gt yr^{-1}). Nevertheless, these glaciers have the potential to develop widespread melting ponds and build up moraine-dammed lakes (Ageta et al., 2000; Sakai et al., 2000; Quincey et al., 2009).

Three types of glacial lakes can be distinguished according to Ageta et al. (2000): (*i*) lakes that are not directly connected with glaciers but that may have a glacier located in their basin, referred to in this paper as *unconnected glacial lakes*; (*ii*) *supraglacial lakes* (melting ponds), which develop on the surface of the glacier downstream; or (*iii*) *proglacial lakes*, which are moraine-dammed lakes that are in contact with the glacier front. Some of these lakes store large quantities of water and are susceptible to GLOFs (glacial lake outburst floods).

Little is known about the conditions of formation, distribution and evolution of all of these three types of glacial lakes in the southern

* Corresponding author at: IRSA-CNR Via Del Mulino 19, Località Occhiate 20861 Brugherio (MB), Italy. Tel.: +39 39 21694203; fax: +39 39 2004692.
E-mail address: salerno@irsa.cnr.it (F. Salerno).

0921-8181/$ – see front matter © 2012 Elsevier B.V. All rights reserved.
doi:10.1016/j.gloplacha.2012.04.001

central Himalayas, even though these lakes are a suitable indicator for evaluating the impact of climate change at high elevations (Richardson and Reynolds, 2000; Benn et al., 2001). Gardelle et al. (2010), considering *supraglacial* and *proglacial lakes*, note that the southern side of Mt Everest is the region that is most characterized by glacial lakes in the Hindu Kush-Himalaya. Moreover, these lakes have indicated the largest surface area increase of the lakes in the mountain range, estimated at +33% (1990–2009), and thus indicates that the region is appropriate for this survey.

In this context, the glacier and lake mapping indicates the need to pay attention to the uncertainty of the topographical measurements obtained from remote sensing imagery so that data can be analyzed according to the correct relevance to their accuracy. In addition, multi-temporal analysis usually employs data sources (map and satellite) with different degrees of uncertainty that should be taken into account during temporal comparisons.

The overall aim of this work is to provide an updated and complete outline of the three types of glacial lakes and glaciers in the southern region of Mt Everest (October 2008). Considering that these types of measurements are essential in recent studies of the impact of climate change, the analysis on uncertainty of measurements is discussed with the aim of proving this to be a reference study that can be used when glaciers and lakes are measured using remote sensing imagery. Moreover, the attention is focused on the conditions of the formation of glacial lakes, specifically, *unconnected* and *supraglacial lakes*.

2. Study area

The current study is focused on the Everest-region and in particular in the Sagarmatha (Mt Everest) National Park (SNP), the highest protected mountainous area in the world, situated in Solu-Khumbu District in the north-eastern region of Nepal (Fig. 1). This area includes the upper catchment of the Dudh Koshi River Basin which is the part of the Koshi River Basin (or Sapta Koshi River Basin), one of the three large river basins of Nepal. The northern part of the park bounds with the Autonomous Region of Tibet (China). The SNP covers an area of 1148 km^2 encompassing altitudes from 2845 m (at Jorsale) to 8848 m at the summit of Mount Everest (Sagarmatha in Nepali). The park falls between latitude 27°45'00″ to 28°06′36″ N and longitude 85°58'48" to 86°30'36" E (Salerno et al., 2010; Lami et al., 2010). Land cover classification shows that almost one-third of the territory is characterized by snow and glaciers, while less than 10% of the park area is forested (Bajracharya et al., 2010).

The glaciers in Everest-region show morphological features common to glaciers throughout the Himalayas. Nearly all (28 out of a total of 29) are debris-covered glaciers; these are glaciers in which the ablation zone is almost entirely covered by surface debris that significantly alters the energy exchanges between the ice and the atmosphere (Mattson et al., 1993.). Because the minimum threshold for considering glacier areas in this study was set at 1 km^2 (Supplementary material 1) the only debris-free glacier we consider is Langmuche glacier (Salerno et al., 2008).

Glacier lakes in this region are very vulnerable to climate change and some of them, like Nare Drangka lake and Dig Tsho lake, have already experienced GLOFs in 1977 and 1985 respectively (Fushimi et al., 1985; Yamada and Sharma, 1993). All glacial lakes plotted in Tartari et al., 2008 on a 1992 map for the north-eastern sector of Everest-region were at between 4460 m and 5560 m in altitude, with the maximum frequency of altitude distribution falling between 5100 m and 5300 m. The lakes were fed prevalently by perennial snow and glaciers, than direct runoff from precipitation. However some lakes were detected without glacial masses in their hydrographic basin. These often prove to be temporary ponds, although in

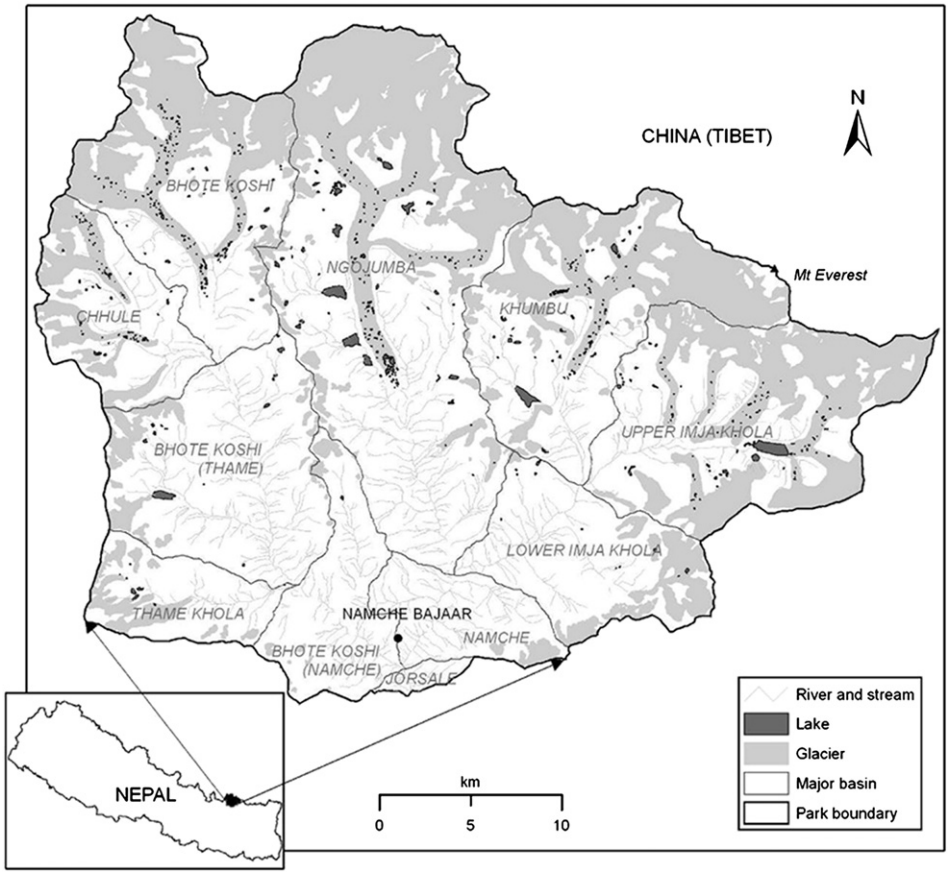

Fig. 1. Location of the study area: Sagarmatha National Park, Nepal.

the case of lakes fed by glaciers and/or snowfields it is not infrequent to observe strong variations in level during the inter-monsoon period (October-March).

3. Data and methods

3.1. Satellite data

Glaciers and lakes were manually identified and digitized using the Advanced Visible and Near Infrared Radiometer type 2 (AVNIR-2) onboard ALOS image, received from a Japanese Earth Observation satellite launched in January 2006. AVNIR-2 is a multispectral radiometer for observing land and coastal zones with a 10 m spatial resolution, a 70 km swath width (at nadir), and a revisiting time of 46 days. AVNIR-2 data investigated in this study were acquired on 24th October 2008 (Scene ID ALAV2A146473040) in a cloudless sky. The image was acquired at the end of the monsoon season before the first heavy snowfall. Image data were orthorectified and corrected for the atmospheric effects using the 6 S code (Vermote et al., 1997; Giardino et al., 2010).

3.2. Uncertainty of measurements

3.2.1. Glacier and lake surfaces

In general the measurement accuracy of the position of a single point or an edge in the space ($n=1$, $i=1$), within the use of the *GIS* (Geographical Information System), is limited by the resolution of the source data used (i.e., cartography, satellite image), which we define LRE_i (Linear Resolution Error) and by the error of referencing with regard to a reference system (RE_i, co-REgistration error or co-georeferencing error).

In this study the *RE* calculated as to the *Official Nepali map* was ±18 m (Salerno et al., 2008). In the case one would compute the error of two measurements of similar quantities ($n=2$) as regards to a unique reference system common to the two source data (for instance a temporal comparison of the point shifting or of the edge by using two satellite images both co-registered as per a topographical map), the overall Linear Error ($LE_{1\text{-}2}$) should be calculated as the root mean square (rms) of the errors related to the two measurements (1), (Ye et al., 2006). The overall *LE* would be lower in the case the source data were co-registered between them, thus reducing the uncertainty to a single co-registration.

$$LE_{1-2} = \sqrt{\sum_{i=1}^{n=2} LRE^2} + \sqrt{\sum_{i=1}^{n=2} RE^2} \quad (1)$$

This approach is the one usually adopted in studies on the evolution (retreat and advance) of the glacial front (Ye et al., 2006; Shangguan et al., 2010).

In the case that the source data is a topographical map, Inghilleri (1974) points out that at the graphical resolution limit an arbitrary value of 0.2 mm can be assigned, based on the threshold visible to the human eye. The level of approximation of a map (*LRE*) is conventionally given by this limit of 0.2 mm multiplied by the scale factor (Inghilleri, 1974; Salerno et al., 2008).

For satellite imagery, the *LRE* is limited by the sensor resolution, i.e. by the pixel resolution (Williams et al., 1997). It is obvious that a higher sampling resolution yields the ability to measure the location of an object more accurately; however it is not obvious just how high a resolution is required for a specified spatial accuracy. Gorman (1996) tackles this problem starting from the assumption that the boundary of an object region is straight within the length it crosses a pixel region, and that the object width is greater than one pixel unit. With these definitions, the precision error with respect to a point on the boundary of a region is defined as the minimum distance between the point and the object edge. Gorman (1996) asserts the precision error is 0.5 pixels that can be added to or subtracted from the measurement of the outside edge of an object. If this is done, the error will range between −0.5 and 0.5, and in the worst case, the error will be 0.5. Within the wide field of application of the GIS, Zhang et al. (2001) state the accuracy of any data derived from the imagery is around 0.5 pixels or better. But in the specific field of the study of temporal variations that Himalayan lakes undergo, Fujita et al. (2009) also assumed an error of ±0.5 pixel. Consequently in this study we also consider half pixel, thus adopting the worst *LRE* (±5 m).

The uncertainty in the measurement of the dimension of a shape (Aerial Error, AE_i) is dependent both upon the linear error $LE_{1\text{-}2}$ and its perimeter, l_i (McMillan et al., 2007; Salerno et al., 2008) (2). As a consequence, the error for large shapes is proportionally smaller than that for small shapes.

$$AE_i = LE_{1-2} \times l_i \quad (2)$$

This approach has been used to define the uncertainty in lake measurement by McMillan et al. (2007), Fujita et al. (2009), and Gardelle et al. (2010). In the calculation of LE_i, these authors exclusively consider the LRE_i, probably considering that the co-registration error RE_i does not play a key role, since they are small-sized shapes and the comparison is not made pixel by pixel, but entity by entity.

By sharing the approach to exclude the co-registration error, in this study the AE_i for the lakes has been calculated following the Eq. (3). It can be noticed that in the equation the *LRE* relative to a hypothetic comparison with a second measurement with the same error is also calculated (Williams et al., 1997).

$$AE_i = \left(\sqrt{\sum_{i=1}^{n=2} LRE^2}\right) \times l_i = \left(LRE_i\sqrt{2}\right) \times l_i \quad (3)$$

In regard to the error made in the estimation of the glaciers' extension, in this study we thought it correct to use the canonical equation of the AE_i computation (3), considering the larger dimensions as regards the lakes (Silverio and Jaquet, 2005).

3.2.2. The digital elevation model

The digital elevation model (DEM) was created by digitizing the contours of the 1992 map. The interpolation was performed using the kriging method, setting a pixel dimension of 20 m × 20 m. To judge the uncertainty of the interpolation method, 100 map control points were used for validation, obtaining an average absolute difference of 6.3 m. In the application to surface gradient calculations, the measurements are based on the relative values between DEM pixels, and therefore the accuracy of the absolute values is less important (Quincey et al., 2007) and can be disregarded. Consequently, the uncertainty related to the slope calculated using this DEM is also neglected.

To explain *supraglacial lake* distribution as a function of explanatory predictors, we divided the glacier into upstream and downstream zones relative to their slope. To this end, we applied the *CuSum* (cumulative sum) control chart statistical technique to detect the changing point of the glacier slope along the glacier's longitudinal profile. The *CuSum* control chart is a sequential analysis technique used in various disciplines for monitoring change detection. It provides comparative information that can be useful in series analysis (in our case, the hypsographic curve) to identify potential changes in trend means (in our case, a change in glacier slope). The test is relatively powerful in comparison with other tests (Buishand, 1982) for a change-point that occurs toward the center of the time series (Kundzewicz and Robson, 2004). We used the techniques described by Taylor (2000) that combine the use of *CuSum* charts and a bootstrapping technique to compute 1000 iterations of the *CuSum* chart.

4. Results

4.1. Glacier distribution

A total of 29 glaciers accounting for nearly the entire glacier area in the Mount Everest region (97%) was plotted. Supplementary material 1 describes criteria for glacier identification and cataloging. Table 1 shows the morphometric characteristics of each glacier in 2008, and Table 2 provides a general summary of the main features of the glaciers. We observe that the total glacier area is 356.2 (±2%) km^2. The largest glacier is Ngojumba Glacier, with an area of 98.8 (±1%) km^2.

The average aspect of the glaciers is 172.7°; in other words the glaciers are, on average, oriented toward the south. Specifically, Nare and Ama Dablam glaciers are exposed to the west, Cholo, Kdu_gr 38 and Langmuche Glacier to the east, and the remaining majority of the glacier surfaces are exposed mainly to the south. The average glacier slope is 25.8%. The two extremes are Melung, with the lowest average slope (8.5%), and Phunki Glacier, with the highest average slope (44.0%).

Fig. 2 shows the frequency distribution of glaciers relative to their elevation. The glaciers present a mean elevation of the glacial fronts (minimum glacier elevation) of 4900 m (standard deviation 5%), a maximum elevation of 6519 m (standard deviation 13%) and in general a mean elevation of 5487 m (standard deviation 5%). Chhule Glacier has the lowest elevation (4832 m), and Khumbu Glacier has the highest average elevation (6154 m).

4.2. Lake distribution

The first step in creating the lakes cadastre involved analyzing the surface hydrographic network plotted on the 1992 map. This analysis led to the identification of 9 sub-basins of the Dudh Koshi River, which were by convention given the name of their largest associated glacier or the main tributary: Thame Khola and Bhote Koshi River (at Thame) basins, Chhule Glacier and Bhote Koshi Glacier basins, Ngojumba Glacier basin, Khumbu Glacier and Upper Imja Khola basins, and Lower Imja Khola and Bhote Koshi River (at Namche) basins (Supplementary material 2). Supplementary material 1 describes in detail the criteria for lake identification and cataloging.

The total number of lakes plotted in 2008 is 624, corresponding to an overall surface of 7.43 (±18%) km^2. Of these lakes, the *unconnected glacial lakes* are the most frequently represented typology (170 lakes with a total surface of 4.28 (±14%) km^2 equivalent to 58% of the overall lake surface). The second typology in terms of area is represented by the *proglacial lakes* (17 lakes with a total surface of 1.76 (±7%) km^2 equivalent to 24%), while the *supraglacial lakes* typology shows the highest number of water bodies (437 lakes with a total surface of 1.39 (±45%) km^2 equivalent to 18%). This last typology consequently presents the lowest median size for each lake (0.001 km^2), but with a high standard deviation (0.007 km^2). The *unconnected glacial lakes* show a median surface 6 times higher (0.006 km^2), with a proportionally similar standard deviation (0.076 km^2). Finally, the *proglacial lakes* are clearly larger in size compared with the other two typologies (0.025 km^2), and in this case as well, the standard deviation is more than twice the mean (0.245 km^2). Fig. 3 shows the frequency distribution of lakes relative to their area. It can be noted that this distribution for each typology is far from normality (lognormal), with an abundance of small lakes and few large lakes. In addition, although the *supraglacial lakes* show a *kurtosis* of 79, the *proglacial* and *unconnected glacial lakes* have a lower *kurtosis* value (11) and, thus, a frequency distribution highlighting a wider dimensional range compared to the *supraglacial lakes* (Joanes and Gill, 1998).

Fig. 2 shows the frequency distribution of glaciers and lakes relative to their altitude. Starting with the *supraglacial lakes*, we notice

Table 1
Morphometric characteristics of the glaciers and supraglacial lakes of Sagarmatha National Park in 2008 (Up = glacier upstream; Down = glacier downstream; Tot = all glaciers).

Glacier name	Glacier features								Supraglacial lakes features					
	Glacier surface	Aspect	Slope			Elevation a.s.l.			Number of lakes	Elevation a.s.l.		Lakes perimeter	Lakes surface	
	Total	Mean	Up	Down	Mean	Mean	Min	Max	Total	Mean	Stand. Dev.	Total	Total	Density
	(km^2)	(°)	(°)	(°)	(°)	(m)	(m)	(m)	N	(m)	(m)	(km)	(km^2)	(%)
Ama Dablam	9.8	255	37	11	26	5416	4786	6328	8	4976	60	1.76	0.023	0.57
Bhote Koshi	41.6	164	38	10	22	5526	4797	6825	100	5111	136	17.57	0.227	0.92
Chhuitingpo	6.5	148	31	17	27	5618	5105	6199	0					
Chhule	3.1	101	34	7	22	5091	4802	5812	21	4916	77	4.81	0.077	1.81
Cholo	1.4	87	44	13	21	4832	4451	5536	0					
Cholotse	1.5	247	40	13	20	5102	4868	5519	2	4991	90	0.40	0.005	0.46
Duwo	2.1	239	45	9	28	5115	4747	6039	1	4776		0.39	0.008	0.84
Imja	35.1	198	39	12	31	5787	4997	7719	24	5136	62	5.18	0.066	0.65
Kdu_gr 125	1.0	150	32	13	20	5529	5374	5713	0					
Kdu_gr 181	0.6	254	45	26	41	5551	4943	6348	0					
Kdu_gr 38	0.8	82	42	21	40	5700	4944	6532	0					
Khangri	18.5	153	41	9	21	5570	5143	6812	30	5205	20	6.84	0.098	0.82
Khumbu	38.4	206	37	8	29	6154	4907	8199	32	5054	116	7.13	0.108	1.01
Kyajo	1.0	103	33	12	15	5397	5262	5582	0					
Langdak	2.1	103	27	11	18	5259	4785	5810	0					
Langmuche	2.9	83	46	25	43	5639	4456	6788	0					
Lhotse	15.4	210	48	12	28	5807	4854	8254	21	5100	57	3.76	0.046	0.55
Lobuje	1.7	143	26	8	20	5366	4978	5911	2	4992	1	0.68	0.012	2.07
Lumsamba	19.3	179	37	10	25	5860	4937	7272	28	5105	146	6.84	0.087	0.99
Machhermo	1.2	148	29	11	23	5520	5190	5795	0					
Melung	3.7	144	40	10	22	5168	4999	5586	39	5193	114	5.78	0.062	0.86
Nare	6.0	257	32	15	28	5423	4866	6246	0					
Nareyargaip	5.5	217	36	10	23	5512	5149	6157	3	5327	51	1.40	0.048	1.34
Ngojumba	99.8	179	29	9	22	5848	4701	8163	108	4959	199	25.02	0.502	1.32
Nuptse	8.1	205	45	10	28	5758	4963	7764	10	5118	102	1.79	0.023	0.57
Phunki	1.7	206	50	20	45	5390	4853	6329	0					
Thyangbo	8.8	95	36	12	31	5264	4404	6344	1	4621		0.31	0.006	0.32
Tingbo	1.1	254	33	16	29	5148	4922	5867	0					
W. Lhotse	4.5	199	50	9	32	5774	4918	7599	7	5045	60	0.85	0.005	0.29
Other glaciers	12.4								1	5073		0.12	0.001	

Table 2
General summary of the morphometric features of glaciers and lakes divided by typology in the LCN 2008 cadastre.

Glaciers in SNP			Lakes in SNP					
					Proglacial	Supraglacial	Unconnected	All lakes in SNP
Number of glaciers (N)		29	Number of lakes (N)		17	437	170	624
Elevation a.s.l. (m)	Mean	5487	Elevation a.s.l. (m)	Mean	4996	5057	5073	5060
	Max	6154		Max	5660	5394	5484	5660
	Min	4832		Min	4377	4621	3800	3800
	Stand. Dev.	151		Stand. Dev.	307	172	259	199
	Median	5520		Median	4920	5079	5120	5086
Perimeter (km)	Mean	37.9	Perimeter (km)	Mean	1.05	0.20	0.51	0.31
	Max	224.6		Max	4.83	1.77	4.14	4.83
	Min	4.9		Min	0.09	0.04	0.07	0.04
Glacier surface (km^2)	Mean	11.9	Lake surface (km^2)	Mean	0.104	0.003	0.025	0.012
	Max	99.8		Max	0.979	0.086	0.613	0.979
	Min	0.6		Min	0.0006	0.0001	0.0003	0.0001
	Stand. Dev.	20.1		Stand. Dev.	0.245	0.007	0.076	0.032
	Median	3.7		Median	0.025	0.001	0.006	0.003
	Total	356.2		Total	1.762	1.389	4.279	7.430
Slope (°)	Mean	25.8	Sub-basins surface (km^2)	Mean	–	–	1.32	–
	Max	44.0		Max	–	–	16.22	–
	Min	8.5		Min	–	–	0.01	–
	Stand. Dev.	8.3		Stand. Dev.	–	–	2.47	–
	Median	25.9		Median	–	–	0.57	–
Basin surface (km^2)	Mean	25.0	Basin surface (km^2)	Mean	–	–	2.12	–
	Max	192.7		Max	–	–	20.81	–
	Min	2.3		Min	–	–	0.01	–
	Stand. Dev.	37.8		Stand. Dev.	–	–	3.61	–
	Median	13.2		Median	–	–	0.86	–
Aspect (°)	Mean	173	Glacier surface in basin (km^2)	Mean	–	–	0.38	–
	Max	257		Max	–	–	3.04	–
	Min	82		Min	–	–	0.00	–
	Stand. Dev.	58		Stand. Dev.	–	–	0.64	–
	Median	179		Median	–	–	0.08	–

that these lakes are located at a mean altitude of 5055 m a.s.l., i.e., 155 m higher than the glacial fronts (25° and 75° percentiles, corresponding to 4950–5190 m, standard deviation 3%). The generic *unconnected glacial lakes* are approximately 80 m higher, within an elevation zone ranging from 4800 to 5300 m (mean 5073 m, standard deviation 5%). In the Mount Everest region, the elevations of all lakes generally range between 4850 and 5250 m (the weighted average elevation of the area is 5080 m).

Concerning the *supraglacial lakes*, Fig. 4 shows a few examples of longitudinal profiles of selected glaciers traced on the DEM following an equidistant line between the lateral glacier margins from the highest peak to the glacier front. To begin we observe the changing points of the surface slope detected by applying the *CuSum* control chart statistical technique. This technique clearly distinguishes the steeper glacier upstream from the flatter glacier downstream. For all of the glaciers, we observed that *supraglacial lakes*, when present, are located below this changing point of slope and also close to it. This type of glacier subdivision appears to be strictly related and most likely functional to the lake distribution. The slopes of glaciers downstream show that the lakes range from 7° to 13° (Table 1). Reynolds (2000) reported that in the Bhutan Himalayas, small isolated ponds could be found up to 10°. For the Mt Everest region, we observed evidence of *supraglacial* ponds for slightly higher slopes. For the same glaciers, the slopes of the glacier upstream range from 26° to 50° (Table 1). These slopes are typical of the southern central Himalayan range, as reported by Scherler et al. (2011).

5. Discussion

5.1. Consideration for uncertainty of measurements

Until the early 1970s, aerial photography was the primary remote sensing technique available for extracting glacier and lake parameters. Medium-resolution satellite data (10–90 m) have been available for cryospheric studies since that time. Among them, we can mention here sensors such as TERRA ASTER and LANDSAT MSS, TM, ETM+ with a mean resolution of 30 m (15–90 m), the SPOT HRVIR, the IRS LISS III and, more recently, the ALOS AVNIR-2 launched in 2006 and used in this study with a resolution of 10 m (2.5-10 m). In addition to these sensors, there are sensors with high resolution (meter and

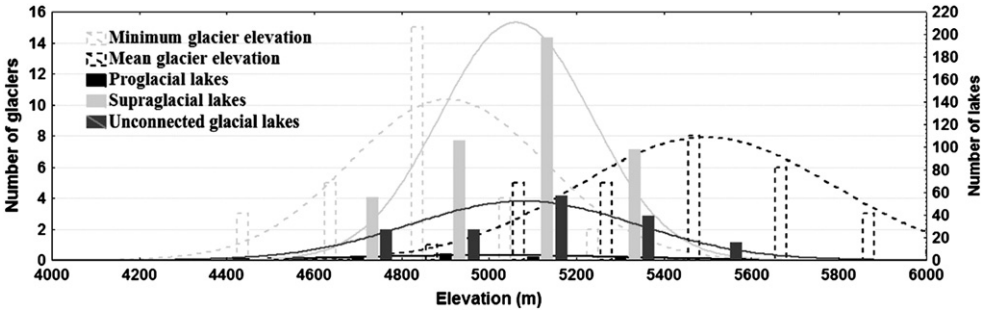

Fig. 2. Frequency distribution of glaciers and lakes relative to their elevation.

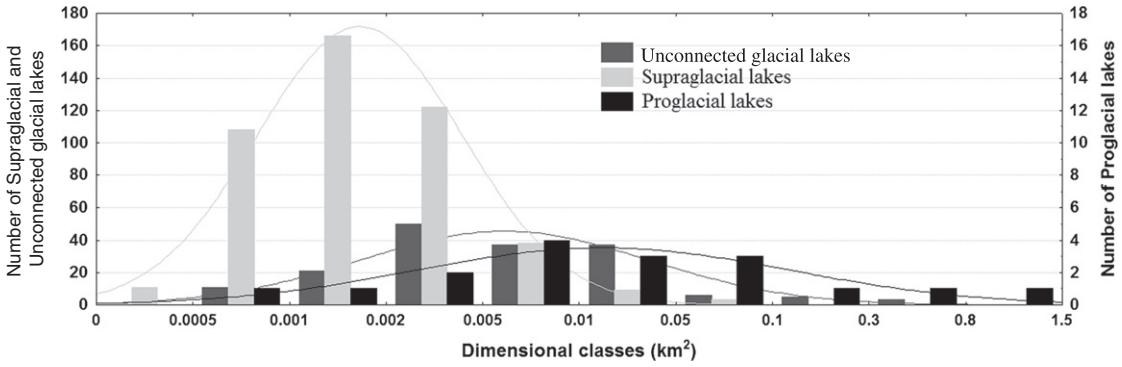

Fig. 3. Frequency distribution of lakes relative to their area and typology.

sub-meter spatial resolution) such as IKONOS, Quickbird and GeoEye-1 (Racoviteanu et al., 2008).

We have noted in this study that the uncertainty in measurement of lake surfaces has been estimated as a function of the sensor resolution and its perimeter according to Eq. (3). As a consequence, the error for large shapes is proportionally smaller than that for small shapes and when sensors with higher resolution are used. In the graph in Fig. 5, we illustrate the relationship between the hypothetic surface of circular lakes and the respective uncertainty of measurement from sensors that differentiate by the degree of resolution. By setting a generic error threshold of 15%, corresponding to the differences observed by Tartari et al. (2008) over a decade, we notice that a high-resolution sensor (1 m) would be able to determine the lake surface with sizes up to and over 0.001 km^2, whereas the dimensional threshold would decrease to 0.01 km^2 for a sensor with a resolution of 5 m, 0.05 km^2 for a sensor with a resolution of 10 m, 0.5 km^2 for a sensor with a resolution of 30 m and 5 km^2 for a sensor with a resolution of 80 m. To simplify, among the resolutions reported in Fig. 5 corresponding to the most common sensors currently available, we notice a capacity of accurately detecting diverging lake sizes by approximately one order of magnitude.

In the following sections, we discuss the conditions of formation of glacial lakes through inference analysis and by weighing the uncertainty as the inverse of the AE_i. The possible significance of the correlations guarantees the uncertainty of measurements considered is sufficiently low for properly describing the relationship.

Concerning the uncertainty in the measurement of glacier surfaces, we noted that, for lakes, the errors are estimated in this study as depending on the sensor resolution and its perimeter according to Eq. (3). For lakes, we compute an overall average *AE* of 18% with a sensor with 10-m resolution; in contrast, using the same sensor, the error associated with glaciers presents a lower order of magnitude (2%). This uncertainty appears to be suitable, considering that Salerno et al. (2008) report that the reduction of the glaciers in terms of surface observed by comparing topographical maps of this region between the 1960s and the 1990s is approximately 5%. If a sensor with 30-m resolution (e.g., LANDSAT TM) was used, the error would become 5%, whereas using a sensor with 80-m resolution (e.g., LANDSAT MSS) would increase the error to 13%, exceeding the magnitude of glacier variations in the region.

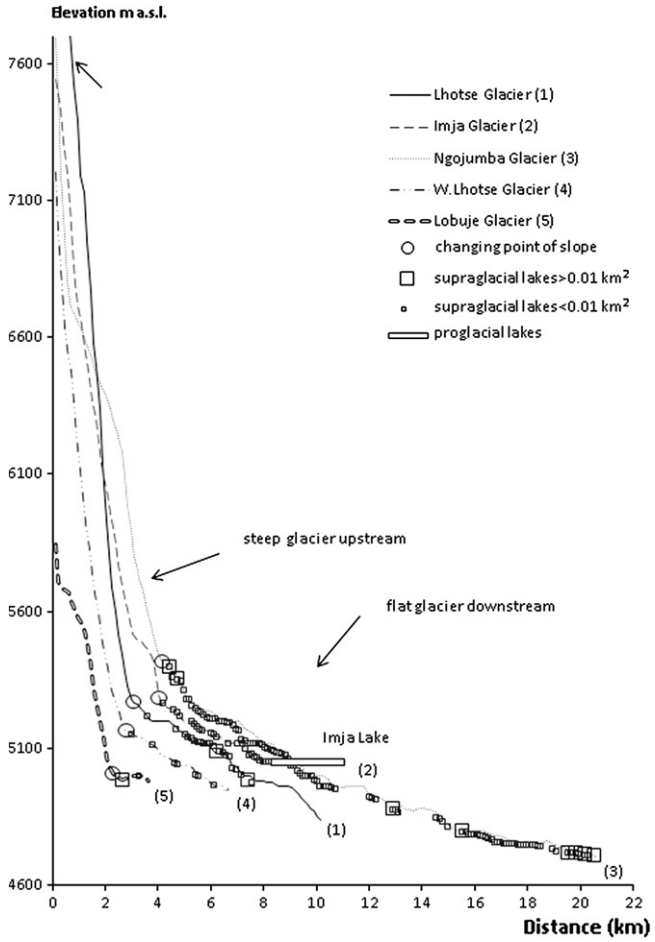

Fig. 4. Elevation profiles of five glaciers in Mt Everest Region. The location of changing point of glacier slopes and *supraglacial lakes* is shown.

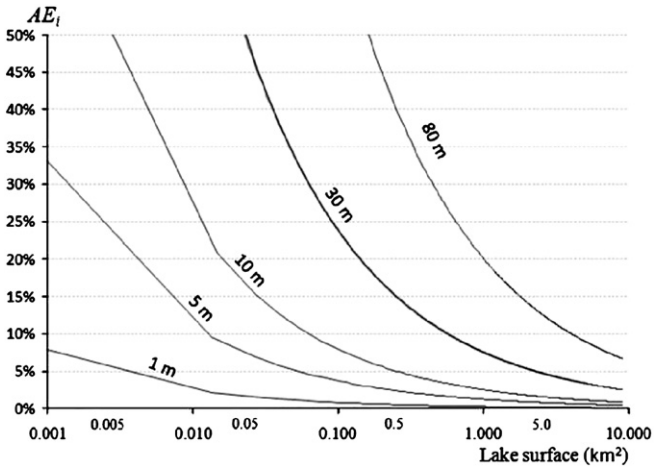

Fig. 5. Relationship between the hypothetical surface of circular lakes and the respective uncertainty of measurement according to sensors that differ by degree of resolution.

5.2. Unconnected glacial lakes

Lakes without direct connections with glaciers (referred to as *unconnected glacial lakes*) are reported without a specific suffix in Supplementary material 3. The median area of the direct drainage sub-basins is found to be 0.57 km^2, whereas if the surfaces of basins belonging to lakes of lower order are included, the area is 0.86 km^2. The size of the basin ranged from 0.01 km^2 for LCN (Lake Cadaster Number) 126 to 20.81 km^2 for LCN 24 (Supplementary material 2 d).

The majority of *unconnected glacial lakes* are located in the Ngojumba Glacier basin: 55 lakes for a total surface of 2.41 ± 11% km^2 (Supplementary material 2 c), corresponding to 56% of *unconnected glacial lakes* of the entire park in terms of area and 32% in terms of number. Moreover, in this basin, the larger lakes, such as LCN 76 with a surface of 0.61 ± 4% km^2, represent the lakes of this typology. Even the Khumbu Glacier basin presents a high number of lakes (30) for a total surface of 0.86 ± 13% km^2 (20% of *unconnected glacial lakes* of the entire park in terms of area and 18% in terms of number). LCN 24 located within the basin of the Khumbu Glacier is the second biggest lake of this typology and has, precisely, a surface of 0.57 ± 5% km^2.

The basins of the *unconnected glacial lakes* have an average glacial surface of 20% in what is considered to be a wide range of contingent situations; indeed, 45% of the lakes do not present glacial surfaces within the basin that directly drains the lake. In this regard, Fig. 6 compares the sub-basin surface and the glacial surface of each basin with the respective lake size. We observe that the lake surface is significantly correlated ($R^2 = 0.62$, $p < 0.001$) with the size of its drainage basin, whereas no correlation is found with the glacial surface ($R^2 = 0.10$, $p > 0.05$). This analysis legitimates the hypothesis that the supply of *unconnected glacial lakes* is determined mainly by the runoff rather than by the glacial melting waters. In fact, the direct proportionality between lake surfaces and their contributing watershed area is evidence that is consistent with the notion that precipitation is the main factor influencing the lake water balance if the evaporation/precipitation ratio is small. In effect, the drainage basin/lake area ratio is related directly to climatic variables of precipitation and evaporation (Sack, 2001; Sack, 2009). Based on the meteorological observations at Pyramid Laboratory-Observatory (2001–2005) located at an elevation of 5050 m and considering that the elevation mean of these lakes is 5073 m, we calculated the evaporation/precipitation ratio. At this high elevation, the annual mean temperature is below 0 °C (−2.5 ± 0.5 °C), and the mean evaporation, applying the Jensen-Haise model for a rough estimation at these altitudes (Gardelle et al., 2010), is 160 ± 6 mm. In our case, the evaporation/precipitation ratio is approximately 0.34 ± 0.07 (mean annual precipitation 490 ± 74 mm). Therefore, a possible variation in precipitation regime affects the lake water balance three times more than the same variation for the evaporation rate. This further evidence allows us to assert that the evolution of these lakes is mainly influenced by the precipitation regime. This remark is critical, considering the current climate change scenario. The monitoring of these lakes thus provides useful indications of the precipitation trend. Similar to this research, we can observe that Fassett and Head (2008), investigating the possible hydrological system of Mars, found that open-basin lakes have volumes that are proportional to their watershed area. These authors considered this evidence to be consistent with what would be expected if the lakes were sourced predominantly by precipitation to their catchments.

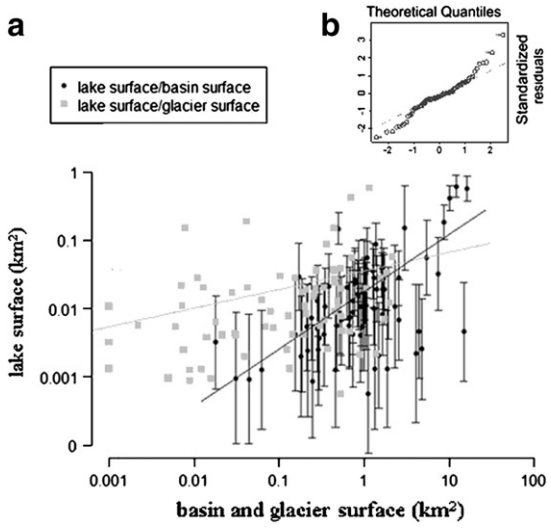

Fig. 6. a) Relationship among the lake sizes, the basin surface and its glacial coverage in the basin. The error bar represents the *AEi*. The linear model is computed considering the inverse of the *AEi* for each lake. b) Normal quantile–quantile plot of residuals of the regression model basin surface/lake sizes.

5.3. Supraglacial lakes

Supraglacial lakes are highly variable in space and time, and their lifetime is unpredictable (Benn et al., 2001). Therefore, as suggested by Gardelle et al. (2010), it is more meaningful and relevant to investigate the conditions of formation considering the total area of these lakes located on a given glacier. Table 1 shows the morphometric characteristics of *supraglacial lakes* grouped by the glacier that each lake belongs to, and Table 2 provides a general statistical summary.

We observe that the majority of lakes are located on the surface of the Ngojumba Glacier (Supplementary material 2 c). Overall, the glacier is associated with more than 100 lakes for a total surface of 0.50 ± 37% km^2. The other glaciers that present a surface clearly interspersed with *supraglacial lakes* are the Bhote Koshi and Khumbu glaciers. In general, 55% of *supraglacial lakes* (60% in terms of surface) of the entire park are situated over these three glaciers. If we consider the total lake surface in respect to the glacier downstream surface of the relevant glacier (Lake Density in Table 1), in general, we can observe that lakes occupy from approximately 0.3 ± 0.1% to 2 ± 0.6% of glacier surfaces. Lobuje and Chhule present the glacier downstream surfaces with the highest relative development of *supraglacial lakes*.

To investigate the controlling parameters of supraglacial lake development further we derived a simple multiple regression model (Fig. 7a). We observed that the mean slope of glacier upstream, the mean slope of glacier downstream and the mean slope of the overall glacier present significant inverse correlations with the *supraglacial lake* surface density, whereas among these predictors, the mutual relationships are less consistent. Even the mean elevation of the glacier downstream is inversely correlated with the *lake* surface density, although at a limited significance level.

All variables were tested for their ability to predict the *lake* surface density. Quadratic terms and interactions were also considered. First, we developed a regression model considering as predictors the mean slope of the overall glacier and the mean elevation of glacier downstream, but this model was able to predict only 47% of *supraglacial lake* surfaces ($R^2 = 0.47$), slightly incrementing the ability of the mean slope of the overall glacier, taken individually, to predict the response variable ($R^2 = 0.40$). The second model tested was between the mean slope of glacier upstream, the mean slope of glacier downstream and the mean elevation of glacier downstream. In this case, the results were definitely better ($R^2 = 0.93$, AIC = −197). The process of model development is conducted with a stepwise simplification through the evaluation of the AIC index. In the final step, we identify the additive model between the mean slope of glacier upstream, the mean slope of glacier downstream and their relevant interaction as the model showing at the same time the highest quality of fit (Fig. 7b) and the lowest number of parameters and equation terms ($R^2 = 0.90$, AIC = −199). The mean elevation of glacier downstream was excluded from this setting because its contribution did

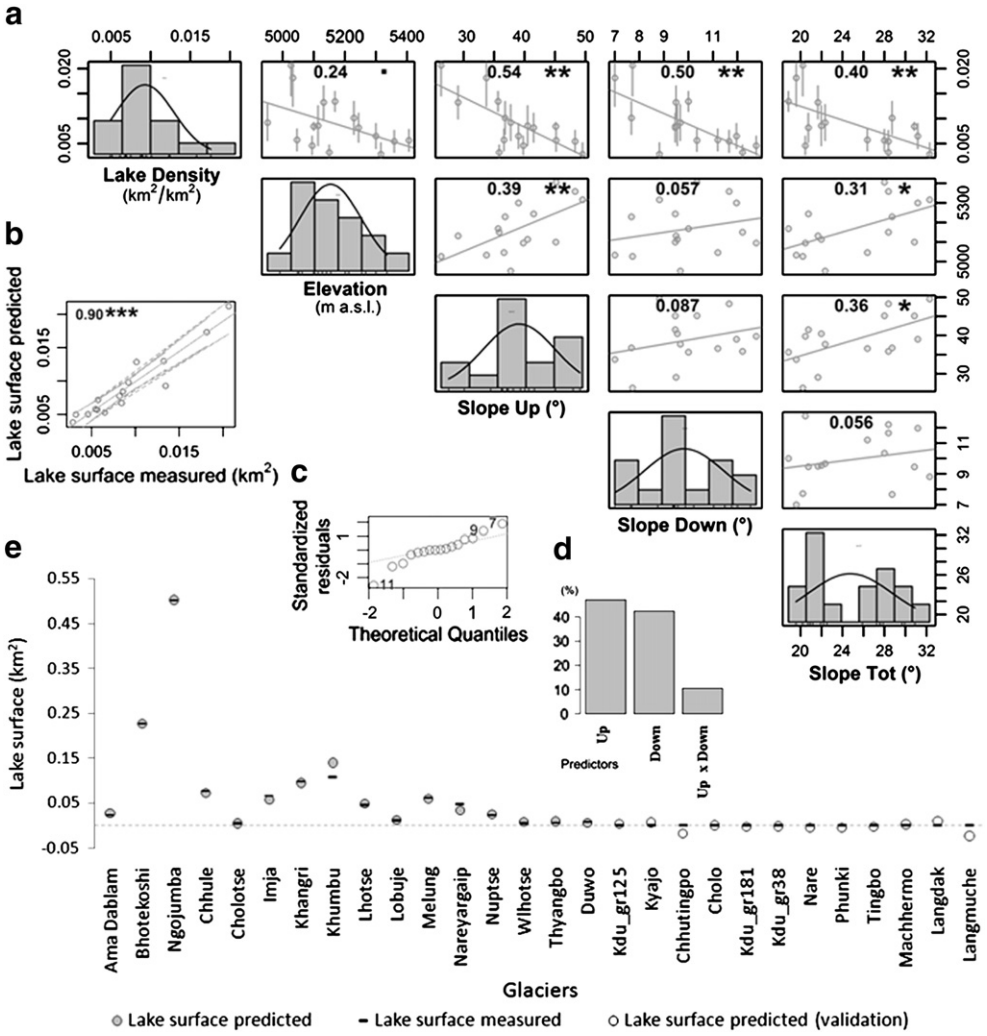

Fig. 7. Multiple regression analysis to explain the supraglacial lake distribution. a) Correlation matrix among predictors and supraglacial lake surface density (Lake Density) (Up = glacier upstream; Down = glacier downstream; Tot = all glacier; Elevation represents the mean elevation of the glacier downstream). For each correlation, the coefficient of determination (R^2) is plotted with a relevant level of significance ($p<0.001$ '***'; $p<0.01$ '**'; $p<0.05$ '*'; $p<0.1$ '.') b) Scatterplot of final regression model relevant confidence levels at 95%. c) Normal quantile-quantile plot of residuals of final regression model. d) Relative importance of the contribution of each predictor for the final regression model (metrics are normalized to sum to 100% of the R^2 of Fig. 7b). e) Comparison between predicted and measured supraglacial lake surfaces for each glacier.

not appear to be significant in improving the predictive ability of the model. Eq. (4) represents the final selected model able to predict the *lake* surface density and consequently the *supraglacial lake* surface of each glacier:

$$LakeSur_i = \left[0.11-(0.0022 * SlopeUp_i)-(0.0088 * SlopeDown_i) + (0.00019 * SlopeUp_i * SlopeDown_i)\right] * SurDown_i \quad (4)$$

where $LakeSur_i$ represents the total *supraglacial lake* surface for each glacier (ith), $SurDown_i$ is the surface downstream of each glacier, and $SlopeUp_i$ and $SlopeDown_i$ refer to the mean slopes of glacier upstream and downstream, respectively. Fig. 7c, presenting the normal quantile–quantile plot of model residuals, shows that the model approaches a normal distribution. Our analysis is completed with a type of further validation applying the model at those glaciers that do not currently present *supraglacial lakes*. Fig. 7e shows a visual evaluation of the estimation of the total *supraglacial lake* surfaces realized by applying the Eq. (4) both at the glaciers used in the calibration phase of the model (full circles) and at the glaciers not presenting lake surfaces (empty circles). We can observe that the model developed can even correctly predict the absence of lakes. In such cases, we obtain negative values that provide an indication of how far the glacier is from developing lakes on its surface. We complete the description of the developed model by discussing the relative contribution of each predictor. Fig. 7d shows that to explain the *supraglacial lake* surfaces, the slope downstream (42%) on which the ponds are located is crucial as well as the slopes upstream (47%) and the interaction of the slopes of these two glacier portions (11%).

Our findings confirm that slope in the glacier area where lakes are located provides the boundary conditions favorable for *supraglacial lake* formation. Reynolds (2000) reports that in the Bhutan Himalaya, small isolated ponds could be found up to 10°. This work demonstrated that where large glacial lakes currently exist, the surface gradient of the glacier prior to lake formation is always less than 2°. These lakes could already be or could evolve to become moraine-dammed lakes (*proglacial* lakes). In our case, having used inferential statistics, the conditions of formation among lakes have to be homogeneous. Therefore, we excluded *proglacial lakes* from this analysis, considering that other variables, as discussed below, can influence their possible development.

Scherler et al. (2011) suggest that lower slopes correspond to lower gravitational driving stresses that, by decreasing the glacier flow, allow the development of stagnant ice, which is a favorable

condition for the formation of lakes. Suzuki et al. (2007), calculating the thermal resistance of debris-covered glaciers, found that those with relatively thin layers of debris tend to develop glacial lakes at their terminus. Sakai and Fujita (2010), analyzing the difference in height between the glacier surface and lateral moraine ridges, observed that the glaciers that record a relatively large decrease in their surface are likely to develop glacial lakes, and therefore, in general, glaciers with high ablation rates tend to develop glacial lakes.

Therefore, the two key factors that appear to be responsible for lake formation are low velocity and high ablation rates at the glacier terminus. Although the mean slope of glacier downstream primarily influences the first requirement, the mean slope of glacier upstream, in our opinion, is able to condition both of these factors. To begin we consider that Scherler et al. (2011) demonstrate that high and deeply incised mountain ranges, in particular in the southern central Himalayas, are responsible for the debris accumulation because the hillslope-erosion rates usually increase with the hillslope angle. The abundance of debris coverage reduces the melt rate of these glaciers, preserving their surfaces from further recession. Therefore, the inverse relationship we found between the mean slope of glacier upstream and lake surfaces favors the formation of lakes because thin debris layers correspond to high ablation rates. Furthermore, we have to consider that many studies highlight the present condition of ice stagnation of glaciers in the Mt Everest region, specifically in the southern central Himalayas, is attributable to low flow velocity generated by a general negative mass balance (Bolch et al., 2008; Quincey et al., 2009; Scherler et al.;, 2011). It is well established that an increase in the glacier flow can be attributed to an increase in the glacier surface slope brought on by an imbalance between the amounts of accumulation versus ablation. This imbalance favors the shear stress on a glacier until it begins to flow. Key factors (boundary conditions) that influence the flow velocity are the slope of the ice as well as the ice thickness and temperature (Cuffey and Paterson, 2010). The greater the top glacier slope, the greater the possibility that an addition of new snow and ice will be transferred to the bottom zone, and therefore higher flow velocity of the glacier termini is expected. Therefore, of two glaciers, the one with a flatter glacier upstream presents more favorable conditions for the development of *supraglacial lakes* caused by a minor transport of debris, which increases the ablation rate, and a minor transport of new snow and ice, which decreases the flow velocity of the glacier termini.

We conclude this analysis by emphasizing that the model that generally considers the overall slope of the entire glacier has a lower capability of predicting the lake distribution because a key factor in determining favorable conditions for lake formation is likely to be the interaction between two glacier zones. The differences between the two glacier zones determine the imbalance, which contributes to the down-slope passage of debris, snow and ice, determining the flow velocity and ablation rate of the glacier termini and consequently the formation conditions for *supraglacial lakes*.

5.4. Proglacial lakes

Supplementary material 3 presents the hydro-morphological features of *proglacial* (suffixed here as *Pro*), while Table 2 provides a general statistical summary. Of the 12 lakes ascribed to this typology, the largest lake is LCN 161, namely, Imja Lake, one of the most studied GLOF-risk lakes in the world (Yamada, 1998; Mool et al., 2001; Bajracharya et al., 2007b; Fujita et al., 2009). In this study, this lake has a surface of $0.98 \pm 3\%$ km^2 (Supplementary material 2 d). The same lake was assessed by Fujita et al. (2009), who found it had a surface of $0.92 \pm 3\%$ km^2 in the same year as our census, although the measurements were performed before the monsoon season and with a sensor of lower resolution (ASTER, 15 m). Another large lake that caused a GLOF event in 1985 is LCN 136, namely, Dig Tsho, which has formed at the foot of the Langmoche Glacier with a surface of $0.40 \pm 5\%$ km^2. At the end of the 1990s, the same lake, studied by Bajracharya et al. (2007a), presented a surface of 0.35 km^2 (0.36 km^2 in 2000 and 0.33 in 2005, according to Bajracharya et al., 2007b) (Supplementary material 2 a).

The formation of *proglacial lakes* is closely connected with the formation of *supraglacial* lakes. Many authors (e.g., Röhl, 2008; Sakai et al., 2009) consider *supraglacial lakes* to be precursors of terminus disintegration by growing and coalescing, to culminate in large *proglacial lakes*. However, these lakes can also disappear from the glacier surface, leaving only a depression behind. Ponds enlarge predominantly by melting, but coalescence of ponds may eventually lead to a calving terminus. Quincey et al. (2007) affirms that while the mean slope of glacier downstream provides the boundary conditions favorable for *supraglacial lake* formation, their growth and therefore the potential to become a large *proglacial lake* depends on local conditions. These researchers suggest that local variations in glacier velocity and surface morphology between flow units control lake growth. Integrating the surface gradient and velocity information into a single analysis, these authors highlight those glaciers that are particularly vulnerable to development as *proglacial lakes*.

In this study, we contribute to defining the conditions of formation of *supraglacial lakes* and therefore of *proglacial* ones, although we agree with the authors mentioned that the enlargement phenomena of these lakes need to be explained at a lower scale, allowing the peculiarity of single lakes to emerge (Hambrey et al., 2008; Röhl, 2008).

6. Conclusions

In this study, we use ALOS imagery (October 2008) with a medium-high resolution (10 m) for a concomitant hand mapping of glaciers and lakes of the entire southern side of the Mt Everest region. We examined 29 glaciers and 624 lakes (17 *proglacial*, 437 *supraglacial* and 170 *unconnected glacial lakes*). Our attention was focused on the conditions of the formation of lakes, examining the relationship between local basin topography, glacier features and lake dimensions.

The results confirm that the slope of the glacier where lakes are located influences the *supraglacial lake* formation. Moreover, this study is novel in highlighting a further boundary condition. The slope of glacier upstream favors the formation of *supraglacial* lakes because of the minor transport of debris, which increases the ablation rate, and the minor transport of new snow and ice, which decreases the flow velocity of the glacier termini. The regression model developed here has been tested in the most representative comparison of processes that determine the formation of *supraglacial* lakes (Scherler et al., 2011; Gardelle et al., 2010). Nevertheless, the model does not aim to predict the behavior of future lakes but rather encourages further testing in similar environments (debris-covered glaciers) for evaluating possible different behaviors.

The formation of *proglacial lakes* is closely connected with the formation of *supraglacial* ones. These lakes are indeed considered to be precursors of terminus disintegration by growing and coalescing, to culminate in large *proglacial lakes.* However, the enlargement phenomena of these lakes could be explained only on a local scale, thus allowing the peculiarity of the single lake to emerge.

Moreover, these high altitudes are characterized by a significant presence of *unconnected glacial lakes*. Although these bodies of water have been neglected to date, we found they can provide useful indications on the precipitation trend in these remote areas. Our analysis has been completed by an accurate assessment of the uncertainties of topographical measurements made by remote sensing imagery. The results highlight that medium-resolution sensors (10 m) are able to describe lake and glacier surfaces correctly and possibly their variations in the case of multi-temporal analysis, although a direct comparison between lakes needs to be confined to the largest ones. The use of lower resolution sensors could highlight greater uncertainty than the observed evolutions. Regarding glaciers,

the error associated with the estimation of their surfaces presents a lower order of magnitude than that associated with the lakes, thus correctly characterizing the entire resource.

Supplementary data to this article can be found online at http://dx.doi.org/10.1016/j.gloplacha.2012.04.001.

Acknowledgments

The study was conducted by IRSA-CNR and University of Milan within the framework of the Ev-K2-CNR and Nepal Academy of Science and Technology joint research project in Nepal under the terms of the Memorandum of Understanding between Nepal and Italy, with the support of the Italian National Research Council and the Italian Ministry of Foreign Affairs. ALOS AVNIR-2 data were acquired within the ESA AO553 MELINOS Project.

References

Ageta, Y., Iwata, S., Yabuki, H., Naito, N., Sakai, A., Narama, C., Karma, T., 2000. Expansion of glacier lakes in recent decades in the Bhutan Himalayas. IAHS Publication, 264, pp. 165–175.

Bajracharya, B., Shrestha, A.B., Rajbhandari, L., 2007a. Glacial lake outburst floods in the Sagarmatha region- hazard assessment using GIS and hydrodynamic modeling. Mountain Research and Development 27 (4), 336–344.

Bajracharya, S.R., Mool, P.K., Shrestha, B.R., 2007b. Impact of climate change on Himalayan glaciers and glacial lakes. ICIMOD/UNEP Publication. 119 pp.

Bajracharya, B., Uddin, K., Chettri, N., Shrestha, B., Siddiqui, S.A., 2010. Understanding land cover change using a harmonized classification system in the Himalayas: A case study from Sagarmatha National Park, Nepal. Mountain Research and Development 30 (2), 143–156.

Benn, D.I., Wiseman, S., Hands, K.A., 2001. Growth and drainage of supraglacial lakes on debris-mantled Ngozumpa Glacier, Khumbu Himal, Nepal. Journal of Glaciology 47 (159), 177–185.

Bolch, T., Buchroithner, M., Pieczonka, T., Kunert, A., 2008. Planimetric and volumetric glacier changes in the Khumbu Himal, Nepal, since 1962 using Corona, Landsat TM and ASTER data. Journal of Glaciology 54, 592–600.

Buishand, T.A., 1982. Some methods for testing the homogeneity of rainfall records. Journal of Hydrology 58, 11–27.

Cuffey, K.M., Paterson, W.S.B., 2010. The Physics of Glaciers, 4th edition. Elsevier, Inc.. 704 pp.

Fassett, C.I., Head III, J.W., 2008. Valley network-fed, open-basin lakes on Mars: Distribution and implications for Noachian surface and subsurface hydrology. Icarus 198, 37–56.

Fujita, K., Sakai, A., Nuimura, T., Yamaguchi, S., Sharma, R., 2009. Recent changes in Imja Glacial lake and its damming moraine in the Nepal Himalaya revealed by in situ surveys and multi-temporal ASTER imagery. Environmental Research Letters 4, 1–7.

Fushimi, H., Ikegami, K., Higuchi, K., Shankar, K., 1985. Nepal case study: Catastrophic floods. AHS Publication, 149, pp. 125–130.

Gardelle, J., Arnaud, Y., Berthier, E., 2010. Contrasted evolution of glacial lakes along the Hindu Kush Himalaya mountain range between 1990 and 2009. Global and Planetary Change 75 (1–2), 47–55.

Giardino, C., Oggioni, A., Bresciani, M., Huimin, Y., 2010. Remote sensing of suspended particulate matter in Himalayan lakes: A case study of Alpine lakes in the Mount Everest region. Mountain Research and Development 30 (2), 157–168.

Gorman, L.O., 1996. Subpixel precision of straight-edged shapes for registration and measurement. IEEE Transactions on Pattern Analysis and Machine Intelligence 18 (7), 746–751.

Hambrey, M.J., Quincey, D.J., Glasser, N.F., Reynolds, J.M., Richardson, S.J., Clemmens, S., 2008. Sedimentological, geomorphological and dynamic context of debris mantled glaciers, Mount Everest (Sagarmatha) region, Nepal. Quaternary Science Reviews 27, 2361–2389.

Inghilleri, G., 1974. Topografia generale. UTET Publication, Torino. 445 pp.

Jacob, T., Wahr, J., Pfeffer, W.T., Swenson, S., 2012. Recent contributions of glaciers and ice caps to sea level rise. Nature 482, 514–518.

Joanes, D.N., Gill, C.A., 1998. Comparing measures of sample skewness and kurtosis. Journal of the Royal Statistical Society Series D: The Statistician 47 (1), 183–189.

Kundzewicz, Z.W., Robson, A.J., 2004. Change detection in hydrological records—a review of the methodology. Hydrological Sciences Journal 49 (1), 7–19.

Lami, A., Marchetto, A., Musazzi, S., Salerno, F., Tartari, G., Guilizzoni, P., Rogora, M., Tartari, G.A., 2010. Chemical and biological response of two small lakes in the Khumbu Valley, Himalayas (Nepal) to short-term variability and climatic change as detected by long-term monitoring and paleolimnological methods. Hydrobiologia 648, 189–205.

Mattson, L.E., Gardner, J.S., Young, G.J., 1993. Ablation on debris covered glaciers: an example from the Rakhiot Glacier, Panjab, Himalaya. IAHS Publication, 218, pp. 289–296.

McMillan, M., Nienow, P., Shepherd, A., Benham, T., Sole, A., 2007. Seasonal evolution of supra-glacial lakes on the Greenland Ice Sheet. Earth and Planetary Science Letters 262, 484–492.

Mool, P.K., Bajracharya, S.R., Joshi, S.P., 2001. Inventory of glaciers, glacial lakes and glacial lake outburst floods: monitoring and early warning systems in the Hindu Kush–Himalayan region, Nepal. ICIMOD/UNEP Publication. 197 pp.

Quincey, D.J., Richardson, S.D., Luckman, A., Lucas, R.M., Reynolds, J.M., Hambrey, M.J., Glasser, N.J., 2007. Early recognition of glacial lake hazards in the Himalaya using remote sensing datasets. Global and Planetary Change 56 (1–2), 137–152.

Quincey, D.J., Luckman, A., Benn, D., 2009. Quantification of Everest region glacier velocities between 1992 and 2002, using satellite radar interferometry and feature tracking. Journal of Glaciology 55 (192), 596–606.

Racoviteanu, A.E., Williams, M.W., Barry, R.G., 2008. Optical remote sensing of glacier characteristics: A review with focus on the Himalaya. Sensors 8, 3355–3383.

Reynolds, J.M., 2000. On the formation of supraglacial lakes on debris-covered glaciers. IAHS publications, 264, pp. 153–161.

Richardson, S., Reynolds, J., 2000. An overview of glacial hazards in the Himalayas. Quaternary International 65–66, 31–47.

Röhl, K., 2008. Characteristics and evolution of supraglacial ponds on debris-covered Tasman Glacier, New Zealand. Journal of Glaciology 54 (188), 867–880.

Sack, D., 2001. Shoreline and basin configuration techniques in paleolimnology. In: Last, W.M., Smol, J.P. (Eds.), Tracking Environmental Change Using Lake Sediments. Basin Analysis, Coring, and Chronological Techniques, 1. Kluwer Academic Publishers, pp. 49–72.

Sack, D., 2009. Evidence for climate change from desert basin palaeolakes. In: Parsons, A.J., Abrahams, A.D. (Eds.), Geomorphology of desert environments. Springer, Dordrecht, The Netherlands, pp. 743–756.

Sakai, A., Fujita, K., 2010. Formation conditions of supraglacial lakes on debris-covered glaciers in the Himalaya. Journal of Glaciology 56 (195), 177–181.

Sakai, A., Takeuchi, N., Fujita, K., Nakawo, M., 2000. Role of supraglacial ponds in the ablation process of a debriscovered glacier in the Nepal Himalayas. IAHS Publication, 264, pp. 119–130.

Sakai, A., Nishimura, K., Kadota, T., Takeuchi, N., 2009. Onset of calving at supraglacial lakes on debris covered glaciers of the Nepal Himalayas. Journal of Glaciology 55 (193), 909–917.

Salerno, F., Buraschi, E., Bruccoleri, G., Tartari, G., Smiraglia, C., 2008. Glacier surface-area changes in Sagarmatha National Park, Nepal, in the second half of the 20th century, by comparison of historical maps. Journal of Glaciology 54 (187), 738–752.

Salerno, F., Viviano, G., Thakuri, S., Flury, B., Maskey, R.K., Khanal, S.N., Bhuju, D., Carrer, M., Bhochhibhoya, S., Melis, M.T., Giannino, F., Staiano, A., Carteni, F., Mazzoleni, S., Cogo, A., Sapkota, A., Shrestha, S., Pandey, R.K., Manfredi, E.C., 2010. Energy, forest, and indoor air pollution models for Sagarmatha National Park and Buffer zone, Nepal: Implementation of a participatory modeling framework. Mountain Research and Development 30 (2), 113–126.

Scherler, D., Leprince, S., Strecker, M.R., 2008. Glacier-surface velocities in alpine terrain from optical satellite imagery-Accuracy improvement and quality assessment. Remote Sensing of Environment 112, 3806–3819.

Scherler, D., Bookhagen, B., Strecker, M.R., 2011. Spatially variable response of Himalayan glaciers to climate change affected by debris cover. Nature Geoscience 4, 156–159.

Shangguan, D., Liu, S., Ding, Y., Zhang, Y., Li, J., Li, X., Wu, Z., 2010. Changes in the elevation and extent of two glaciers along the Yanglonghe river, Qilian Shan, China. Journal of Glaciology 56 (196), 309–317.

Silverio, W., Jaquet, J.M., 2005. Glacial cover mapping (1987–1996) of the Cordillera Blanca (Peru) using satellite imagery. Remote Sensing of Environment 95 (3), 342–350.

Suzuki, R., Fujita, K., Ageta, Y., 2007. Spatial distribution of thermal properties on debris-covered glaciers in the Himalayas derived from ASTER data. Bulletin of Glaciological Research 24, 13–22.

Tartari, G., Salerno, F., Buraschi, E., Bruccoleri, G., Smiraglia, C., 2008. Lake surface area variations in the north-eastern sector of Sagarmatha National Park (Nepal) at the end of the 20th century by comparison of historical maps. Journal of Limnology 67, 139–154.

Taylor, W.A., 2000. Change-Point Analysis: A Powerful New Tool For Detecting Changes. http://www.variation.com/cpa/tech/changepoint.html 2000.

Vermote, E.F., Tanrè, D., Deizè, J.L., Herman, M., Morcrette, J.J., 1997. Second simulation of the satellite signal in the solar spectrum, 6S: An overview. IEEE Transactions on Geoscience and Remote Sensing 35, 675–686.

Williams, R.S., Hall Jr., D.K., Chien, J.Y.L., 1997. Comparison of satellite-derived with ground-based measurements of the fluctuations of the margins of Vatnajokull, Iceland, 1973–92. Annals of Glaciology 24, 72–80.

Yamada, T., 1998. Glacier lake and its outburst flood in the Nepal Himalaya. Monograph No. 1, Data Center for Glacier Research. Japanese Society of Snow and Ice. 96 pp.

Yamada, T., Sharma, C.K., 1993. Glacier lakes and outburst floods in Nepal Himalaya. Snow and Glacier Hydrology: IAHS Publication, 218, pp. 319–330.

Ye, Q., Kang, S., Chen, F., Wang, J., 2006. Monitoring glacier variations on Geladandong mountain, Central Tibetan Plateau, from 1969 to 2002 using remote-sensing and GIS technologies. Journal of Glaciology 52 (179), 537–545.

Zhang, B., Walker, S., Miller, S., 2001. 3D feature extraction from imagery using ArcSDE. Proceedings of ESRI International Users Conference, 2001, San Diego, CA.